SCIENTIFIC REPORTS

OPEN

SUBJECT AREAS:
NANOPORES
METAL-ORGANIC FRAMEWORKS

Received
6 November 2013

Accepted
3 January 2014

Published
3 February 2014

Correspondence and requests for materials should be addressed to N.K.S. (nabeenkhrestha@hotmail.com) or S.-H.H. (shhan@hanyang.ac.kr)

Enhanced photovoltaic performance of Cu-based metal-organic frameworks sensitized solar cell by addition of carbon nanotubes

Deok Yeon Lee[1], Chan Yong Shin[1], Seog Joon Yoon[1], Haw Young Lee[2], Wonjoo Lee[3], Nabeen K. Shrestha[1], Joong Kee Lee[2] & Sung-Hwan Han[1]

[1]Inorganic Nano-materials Lab, Department of Chemistry, Hanyang University, Haengdang-dong 17, Sungdong-ku, Seoul 133-791 (Republic of Korea), [2]Korea Institute of Science and Technology, Seoul 136-791 (Republic of Korea), [3]Department of Defence Ammunitions, Daeduk College, Daejeon 305-715 (Republic of Korea).

In the present work, TiO_2 nanoparticle and multi-walled carbon nanotubes composite powder is prepared hydrothermally. After doctor blading the paste from composite powder, the resulted composite film is sensitized with Cu-based metal-organic frameworks using a layer-by-layer deposition technique and the film is characterized using FE-SEM, EDX, XRD, UV/Visible spectrophotometry and photoluminescence spectroscopy. The influence of the carbon nanotubes in photovoltaic performance is studied by constructing a Grätzel cell with I_3^-/I^- redox couple containing electrolyte. The results demonstrate that the introduction of carbon nanotubes accelerates the electron transfer, and thereby enhances the photovoltaic performance of the cell with a nearly 60% increment in power conversion efficiency.

Metal-organic frameworks (MOFs) are highly porous network materials formed by coordination of metal ions and organic linkers[1–4]. Owing to huge flexibility in selection and coordination of metal ions and organic linkers, infinite varieties of frameworks with tunable geometry, pores and functionality can be produced. By far, MOFs have been investigated mostly in host-guest chemistry- for example, storing some gases needed for future application, adsorption of toxic gases, and as a drug delivery system[5–9]. In addition, they have also been studied for applications in catalysis[10,11], photocatalysis[12–14], and sensors[15], and to some extent in electrochemical devices[16–18]. In recent years, photovoltaics is one of the most investigated areas in materials science. However, investigation on MOFs as photovoltaic materials has been rarely touched[19–26]. Moreover, most of the reports demonstrated only the measurement of photocurrent from a MOF based half cells. Very recently, successful construction and characterization of a fully devised Cu-MOFs based solar cell has been demonstrated although the cell in this case exhibited poor performance[27]. Nevertheless, such investigation is expected to propel this field further into new realms of emerging field in which far more sophisticated photoactive MOF materials suitable for solar cell may be accessed. It has been well demonstrated that incorporation of carbon nanotubes (CNTs) into TiO_2 film in a DSSC provides more efficient electron transfer due to the outstanding electrical properties of CNTs[28–33]. Further, it has also been demonstrated that introduction of CNTs into solar cell enhances the electric field of the devices[34]. All of these phenomena accelerate the electron transfer rate, and thereby enhance the power conversion efficiency of the device. Based on these facts, CNTs were introduced into the Cu-based MOF sensitized solar cell in an attempt to improve the performance of the cell. This enabled us to enhance the power conversion efficiency of the cell by nearly 60%.

Results

Fig. 1 shows the SEM top and cross sectional views of the doctor bladed TiO_2-MWCNTs composite film on a FTO substrate before and after sensitization with MOFs. A well dispersed TiO_2 and CNTs on the coating film can be observed from the SEM image. After 12 layer-by-layer (LBL) cycles, clearly large number of MOF crystals on the coating surface are evident. When the bottom part of the sensitized film is zoomed, 65.2 nm thick hole blocking TiO_2 compact layer on a 539 nm thick FTO coated glass substrate are observed (Fig. 1d). Over this hole blocking

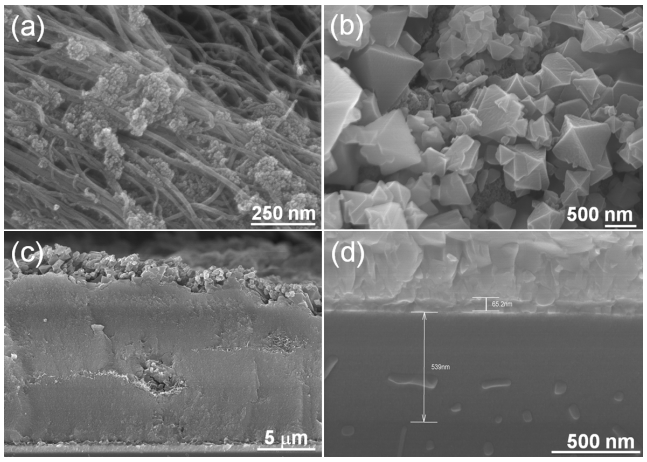

Figure 1 | (a) SEM top views of doctor bladed TiO_2–MWCNTs composite film on a FTO glass. SEM top (b) and cross sectional (c) views of the same film after sensitization with Cu-MOFs for 12 LBL cycles. (d) Magnified view at the bottom of the same sensitized composite film.

layer, presence of the framework entities can be clearly seen. This finding suggests that the deposition of MOFs has reached up to the bottom of the TiO_2-MWCNTs composite film. The composite films before and after MOF sensitization were investigated with EDX. In addition to Ti, O and C (Fig. 2a), which are the structural elements of TiO_2-MWCNTs composite film, the sensitized film also exhibited the presence of Cu (Fig. 2b). This finding reveals the deposition of Cu-MOFs into the composite film. As demonstrated previously[27], conductivity of the Cu-MOFs is close to an insulator and iodine doping is required to modify the conductivity. Therefore, iodine doping into the frameworks of the composite film was carried out in order to improve the conductivity and the charge transfer across TiO_2/MOFs interfaces. The EDX analysis of the iodine doped film is shown in Fig. 2c, which shows the presence of about 2 atomic % of iodine. The composite films were also characterized using XRD and the results are shown in Fig. 2d. As compared to the TiO_2-MWCNTs composite film, the XRD patterns of the film after MOF sensitization are quite different. After sensitization, the film exhibited many additional new XRD signals at around 2 theta = $5^\circ \sim 20^\circ$, which are the characteristic peaks of MOFs[27]. This result confirms the deposition of Cu-MOFs into the TiO_2-MWCNTs composite film.

During sensitization, the color of the film after every LBL cycle turned gradually into blue and blue-green, and finally to dark blue-green at the end of 12 LBL cycles (Fig. S1a, Supplementary information). It should be noted here that the UV/Visible absorption spectrum of the TiO_2-MWCNTs composite film does not show any absorption light especially in visible light regime. However, after sensitizing with Cu-MOFs, the composite film exhibits visible light absorption with the maximum absorption at about 680 nm (Fig. S1b, Supplementary information), which is the characteristic absorption peak of Cu-MOFs[24]. When the MOF sensitized film is illuminated with light at 680 nm, regardless of doping, the MOFs film exhibited highly intense photoluminescence (PL) emission at about 695 nm. However, in the presence of TiO_2-MWCNTs composite film, quantitative quenching of emission is observed (Fig. 3a). Further, when the MOF film deposited on a nonconducting glass substrate was illuminated, as expected no flow of current was observed. However, it is interesting to note that after iodine doping, the MOF film on the nonconducting glass substrate exhibited the flow of photocurrent (Fig. 3b). These results show that MOFs are photoactive but it cannot conduct electricity. In addition to the previously reported findings[27], this result also supports that iodine improves the conductivity of the MOFs dramatically. Fig. 4a shows the current-voltage (J-V) behavior of a MOF sensitized solar cell. As a reference, P25 TiO_2 particle film was also sensitized with the MOFs under similar conditions used for sensitization of doctor bladed hydrothermal TiO_2-MWCNTs composite film. In addition, doctor bladed hydrothermal TiO_2-MWCNTs composite film without sensitization is also investigated, which shows no noticeable photovoltaic performance. The details of various photovoltaic parameters determined from the J-V curves are tabulated in Table 1. From the J-V curves and Table 1, it can be clearly observed that the hydrothermally prepared TiO_2 exhibited a better photovoltaic performance. When MWCNTs were introduced into the TiO_2 film, it exhibited an enhanced photovoltaic performance with the increment of power conversion efficiency by

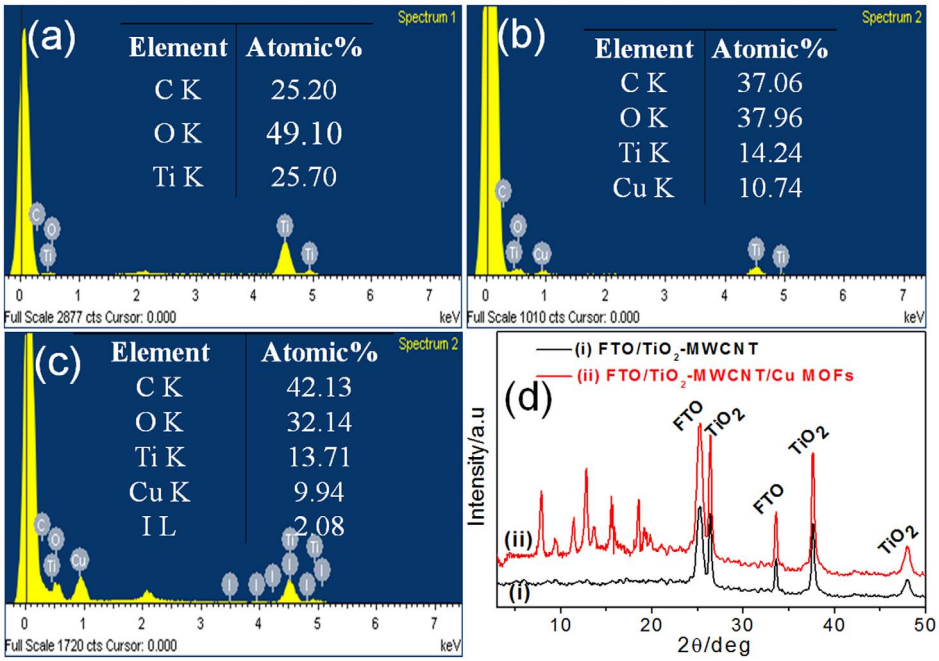

Figure 2 | EDX spectra of doctor bladed (a) TiO_2–MWCNTs composite film, (b) the same film after sensitizing with Cu-MOFs, and (c) the same sensitized film after iodine doping. (d) XRD patterns of the same composite film before (i), and after (ii) sensitization with Cu-MOFs.

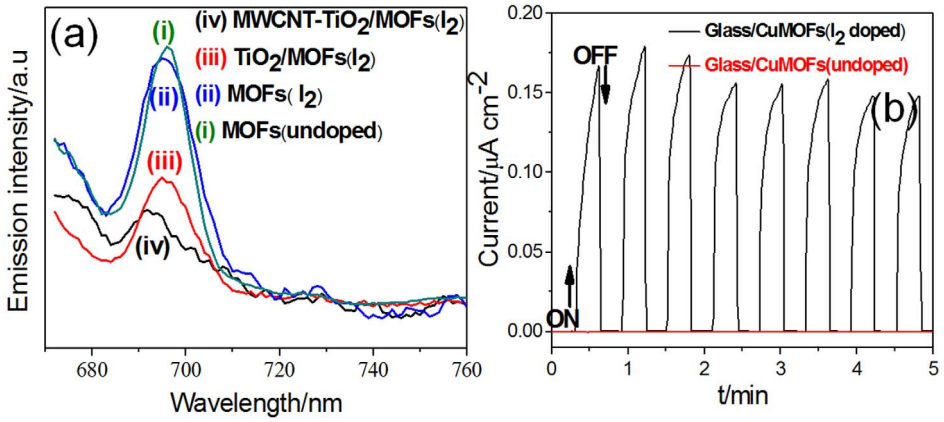

Figure 3 | (a) PL spectra of (i) MOFs (undoped), (ii) MOFs (I_2 doped), (iii) TiO_2/MOFs (I_2 doped), and (iv) MWCNTs-TiO_2/MOFs (I_2 doped) films on a glass substrate. Excitation at 680 nm. (b) Photocurrent transient of undoped and iodine doped Cu-MOFs film on a plain non-conducting glass.

nearly 60%. The incident photon to current efficiency (IPCE) spectrum of the CNTs introduced photoanode is shown in Fig. 4b, which also supports that the MOF layer used in the present study is acting as a sensitizer. The cells were further characterized using impedance spectroscopy and the Nyquist plots are shown in Fig. 5a. As compared to the cell with hydrothermally prepared TiO_2 particles, the larger semicircle demonstrated by the cell with P25 TiO_2 particles reveals its poor interfacial electron transfer between the electrolyte and the MOF sensitized TiO_2 particles film. In contrast, a significant reduction in the size of semicircle after introduction of MWCNTs can be observed. These findings suggest the improvement on interfacial resistance after addition of MWCNTs.

Discussion

The TiO_2-MWCNTs composite film exhibited the absorption of visible light only after sensitizing with MOFs. The absorption of visible light by MOFs is one of the essential conditions for the MOFs to be used as sensitizer. In addition, as in the case of dye sensitized solar cells[35], the photogenerated electrons from the LUMO level of the MOFs are needed to be transferred into the conduction band of TiO_2 (if the sensitizer is used to sensitize TiO_2). Previously, it has been shown that the energy levels of TiO_2 and the Cu-MOFs are well matching for the MOFs to be used as sensitizer of TiO_2[27]. The ability of the MOF sensitizer to transfer photoelectrons from its LUMO level to the conduction band of TiO_2 and the influence of MWCNTs on this electron transfer process is investigated by measuring PL emission. The quantitative quenching of PL emission of the MOFs in presence of TiO_2 demonstrated in Fig. 3a shows that the excited electrons of MOFs can be transferred into the TiO_2 film as well as to the TiO_2-MWCNTs composite film. However, previously it has been demonstrated that Cu-MOFs behave as an insulator and iodine doping is essential to improve the conductivity of the frameworks[27]. During doping, I_2 molecules are expected to be confined into the porous sites surrounded by aromatic rings of the ligand in the frameworks. Due to the intermolecular interactions between I_2 and π-electrons from aromatic rings, such arrangements can result in cooperative electrical conductivity. The improved conductivity facilitates electron transportation from the central metal core of the frameworks to TiO_2 in contact with the frameworks via metal to ligand charge transfer (MLCT). Fig. 3a shows that the charge transfer rate from MOFs to TiO_2 is obviously influenced by the presence of MWCNTs. It should be noted here that the degree of quenching in presence of MWCNTs is higher. This result clearly indicates that the MWCNTs further accelerate the charge transfer across TiO_2/MOFs interfaces. This argument is also well supported by the Nyquist plots shown in Fig. 5a. From the Nyquist plot and the equivalent circuit model shown in inset of Fig. 5a, the charge transfer resistance (R2) between the electrolyte and MOF sensitized P25 TiO_2 interface is found to be 731.3 Ω whereas it is 713.1 Ω for electrolyte and MOF sensitized hydrothermal TiO_2 interface. In contrast, the charge transfer resistance between the electrolyte and MOF sensitized hydrothermal TiO_2–MWCNTs interface is found to be 528.0 Ω. The dramatically reduction of charge transfer resistance after introduction of MWCNTs into TiO_2 clearly shows the beneficial influence of

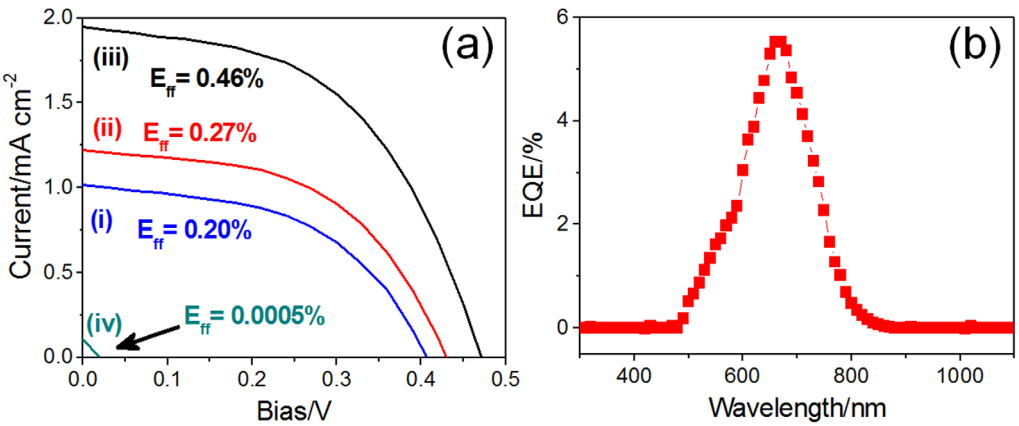

Figure 4 | (a) J-V curve of a cell with the following configurations: (i) FTO-glass/TiO_2 (P25)/Cu-MOF/electrolyte/Pt, (ii) FTO-glass/TiO_2 (hydrothermal)/Cu-MOF/electrolyte/Pt, and (iii) FTO-glass/TiO_2 (hydrothermal)-MW-CNTs/Cu-MOF/electrolyte/Pt. (b) IPCE spectrum of a cell with following configurations: FTO-glass/TiO_2 (hydrothermal)-MW-CNTs/Cu-MOF/electrolyte/Pt.

Table 1 | Photovoltaic performance parameters of Cu-MOF sensitized solar cell

Photoanode	V_{oc}(V)	J_{sc}(mA/cm^2)	FF	E_{FF}(%)
FTO/TiO_2(HBL)/TiO_2(hydrothermal)-MWCNT/MOFs (I_2 doped)	0.48	1.95	0.51	0.46
FTO/TiO_2(HBL)/TiO_2 (hydrothermal)/MOFs (I_2 doped)	0.43	1.22	0.51	0.27
FTO/TiO_2(HBL)/TiO_2(P25)/MOFs (I_2 doped)	0.41	1.01	0.50	0.20

MWCNTs in MOF sensitized solar cells. Due to the outstanding electronic property, the MWCNTs in TiO_2 film act as a network to communicate electronically with all TiO_2 particles in the film, and thus enhance the electron collection efficiency. In addition, they also provide an efficient electronic energy cascade structure[27] as shown in Fig. 5b, which also assists in charge collection efficiency. Further, it has been demonstrated previously that MWCNTs enhance the electric field of the cell[34]. Carbon nanotubes have shown high emission electronic properties due to their good electron conductivity and a high aspect ratio geometry, which amplifies the electrical field strength drastically in the vicinity of the nanotube tip. Therefore, the electric field resulting from the charge separation occurring at the heterogeneous interface (i.e., TiO_2 /MOF/electrolyte interface) of the cell is enhanced by the presence of MWCNTs. The enhanced electric field speeds up the charge transfer process and thereby decreases the recombination process. As a result of these versatile functionalities of the MWCNTs, the electron transfer rate is accelerated, and thereby an enhanced photovoltaic performance of the cell is achieved. This argument is well in line with the increased V_{oc} and J_{sc} as shown in Fig. 4a and Table 1. Meanwhile, it should be noted that without MOF sensitization, the charge transfer resistance for the hydrothermal TiO_2-MWCNTs interface is 258.4 kΩ (Fig. S2, supplementary information), which is 489.4 times larger than when the TiO_2-MWCNTs composite film was sensitized with the MOFs. The smaller charge transfer resistance after sensitization with MOFs under illumination condition indicates the swift charge transfer. In other words, this swift charge transfer means that the MOFs are harvesting light and the photogenerated electrons are pumped into the TiO_2 conduction band as in the case of a dye sensitized solar cell[35]. In addition to the IPCE data, this finding also supports that MOF layer in the present study is working as a sensitizer. Although the efficiency of the MOFs sensitized cell is still lower than the current state of the art in this type of devices, large number of metal ions and variety of organic linkers are available. Therefore, endless coordination between the metal ions and organic linkers are possible to obtain MOFs with different electronic and light harvesting properties, which can further improve the power conversion efficiencies.

In summary, the present work demonstrates that the addition of MWCNTs into TiO_2 particle film improves the interfacial charge transfer resistance significantly. This accelerates the electron transfer rate, and thereby the enhanced photovoltaic performance is achieved. Thus, the introduction of MWCNTs into the Cu-based MOF sensitized TiO_2 particle film of a cell enhanced the power conversion efficiency by nearly 60%.

Methods

Materials. All chemical agents were obtained from manufacturers and used as obtained without further purification. The following chemicals were used in the present study. Titanium isopropoxide: 97%, Alfa Aesar; titanium-diisopropoxide bis (acetyacetonate): 75%, Sigma Aldrich; H_2SO_4: 97%, Matsuneon Chemicals Ltd.; trimesic acid: 98%, Alfa Aesar; $Cu(NO_3)_2.3H_2O$: 99%, Dae Jung Reagent Chemicals; butanol: 99%, Junsei Chemical Co., Ltd; N,N-dimethylformamide (i.e. DMF): 99.8%, Macron Chemicals; acetonitrile: 99%, Burdick & Jackson, and iodine (i.e., I_2): Duksan Chemicals. Multi-walled carbon nanotubes (MWCNTs: CM-100) was purchased from Hanhwa Nanorech, Corp., and fluorine doped tin oxide (FTO, 8 ohm/sq, 77% transmittance in visible range) were obtained from Pilkington TEC Glass.

Preparation of hole blocking layer (HBL) coating. a very thin film (~60 nm) of TiO_2 HBL was coated on a FTO glass by spreading few drops of 0.15 M titanium-diisopropoxide bis (acetyacetonate) in 1-butanol and spinning at 2000 rpm for 30 s. The spin coted sample was annealed at 500°C for 15 min.

Synthesis of TiO_2-MWCNTs composite powder and film. composite powder of TiO_2-MWCNTs was synthesized through hydrothermal approach and its film on a FTO substrate was prepared by doctor blading the composite powder on to the HBL coated FTO glass electrode. The detail procedures can be found elsewhere[33]. In brief, 2 mL titanium isopropoxide was hydrolyzed by adding a sufficient amount of deionized water. Few milligrams of MWCNT was added to the above solution and sonicated for 5 min. After adding 3 mL of H_2SO_4 (1 M), hydrothermal reaction was carried out in a Teflon-lined autoclave vessel at 175°C for 24 h. After washing the precipitate with deionized water and drying at 50°C, grayish TiO_2-MWCNT nanocomposite powder was obtained. This powder was used to prepare a film of the TiO_2-MWCNT nanocomposite on a FTO glass electrode using a doctor blade technique[33].

Sensitization of TiO_2-MWCNTs composite film. sensitization of the composite film was performed by depositing MOFs (i.e., copper (II) benzene-1,3,5-tricarboxylate) using a layer-by-layer (LBL) technique as described previously[27] for 12 LBL cycles. Each LBL cycle is consisted of dipping the HBL coated FTO substrate for 30 min into 0.1 M trimesic acid in DMF solution maintained at 50°C followed by washing the film by dipping it in DMF solution. Subsequently, the acid functionalized FTO substrate is

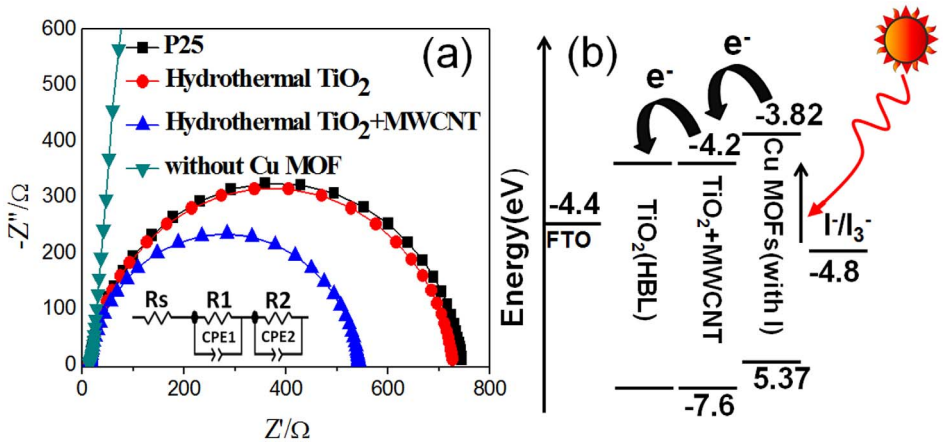

Figure 5 | (a) Impedance spectra of the cell with P25 TiO_2, hydrothermal TiO_2, hydrothermal TiO_2-MWCNTs photoanode sensitized with Cu-MOFs and hydrothermal TiO_2-MWCNTs photoanode without MOF sensitization at open-circuit condition under illumination with simulated AM 1.5 solar radiations. (b) Energy diagram of a TiO_2–MWCNTs/Cu-MOFs system in a solar cell.

dipped into 0.1 M $Cu(NO_3)_2.3H_2O$ in DMF solution maintained at 50°C for 30 min and washing it again in DMF. After desired number of LBL cycles, the MOF sensitized film was dried in Ar-stream and dipped into 0.1 M I_2 in acetonitrile for 2 h in order to dope iodine.

Film characterization. Surface and cross sectional morphologies of the film were obtained using a field enhanced scanning electron microscope (S-4800, Hitachi). EDX analysis was performed using an EDX Micro Analyzer & Detectors (HORIBA) coupled to the scanning electron microscope. XRD patterns were recorded on a D/MAX RINT 2000 diffractometer at 40 KV and 100 mA, using Cu Ka radiation (l 5 1.5406 A°). UV/Vissible spectra were obtained using CARY 100 Conc UV-Visible spectrophotometer, and photoluminescence spectra were recorded using a photoluminescence spectroscope (Photon Counting Spectrofluorimeter-PC1, ISS).

Cell characterization. A sandwich type Grätzel cell was constructed using a polyimide tape as a spacer and a Pt coated FTO glass as a counter electrode. By injecting I_3^-/I^- redox electrolyte (Solanorix) into the cell, current-voltage (I-V) curves were recorded using a computer-controlled digital source meter (Keithley 2400) under illumination of an active area of 0.25 cm^2. The illumination was performed with a solar simulator (PEC-L01, Peccell) under the condition of 100 mW cm^{-2} (1 sun, 1.5 AM). The cell was further characterized by measuring incident photon to current conversion efficiency using K3100 Spectral IPCE Measurement system (McScience), and electrochemical impedance using an electrochemical impedance spectroscopy (IVIUM, COMPACTSAT.e) in the frequency range of 10^{-2} – 10^6 Hz. The measurements of electrochemical impedance were carried out at open-circuit potential at 1 sun condition and the impedance parameters were determined by fitting of impedance spectra using Z-view software.

1. Hoskins, B. F. & Robson, R. Design and construction of a new class of scaffolding-like materials comprising infinite polymeric frameworks of 3D-linked molecular rods. A reappraisal of the zinc cyanide and cadmium cyanide structures and the synthesis and structure of the diamond-related frameworks $[N(CH_3)_4][CuIZnII(CN)_4]$ and CuI[4,4′,4″,4‴ tetracyanotetraphenylmethane]$BF_4.xC_6H_5NO_2$. *J. Am. Chem. Soc.* **112**, 1546–1554 (1990).
2. Li, H., Eddaoudi, M., O'Keeffe, M. & Yaghi, O. M. Design and synthesis of an exceptionally stable and highly porous metal-organic framework. *Nature* **402**, 276–279 (1999).
3. Kitagawa, S., Kitaura, R. & Noro, S. Functional Porous Coordination Polymers. *Angew. Chem. Int. Ed.* **43**, 2334–2375 (2004).
4. Furukawa, H., Cordova, K. E., O'Keeffe, M. & Yaghi, O. M. The Chemistry and Applications of Metal-Organic Frameworks. *Science* **341**, 1230444–1230456 (2013).
5. Chae, H. *et al.* A route to high surface area, porosity and inclusion of large molecules in crystals. *Nature* **427**, 523–527 (2004).
6. Zhao, X. *et al.* Hysteretic Adsorption and Desorption of Hydrogen by Nanoporous Metal-Organic Frameworks. *Science* **306**, 1012–1015 (2004).
7. Sumida, K. *et al.* Carbon Dioxide Capture in Metal–Organic Frameworks. *Chem. Rev.* **112**, 724–781 (2012).
8. Rosseinsky, M. J. Recent developments in metal–organic framework chemistry: design, discovery, permanent porosity and flexibility. *Microporous Mesoporous Mater.* **73**, 15–30 (2004).
9. Rocca, J. D., Liu, D. & Lin, W. Nanoscale Metal–Organic Frameworks for Biomedical Imaging and Drug Delivery. *Acc Chem. Res.* **44**, 957–968 (2011).
10. Lee, J. Y. *et al.* Metal–organic framework materials as catalysts. *Chem. Soc. Rev.* **38**, 1450–1459 (2009).
11. Li, B. *et al.* A strategy toward constructing a bifunctionalized MOF catalyst: post-synthetic modification of MOFs on organic ligands and coordinatively unsaturated metal sites. *Chem. Commun* **48**, 6151–6153 (2012).
12. Wang, C., Xie, Z., DeKrafft, K. E. & Lin, W. Doping Metal–Organic Frameworks for Water Oxidation, Carbon Dioxide Reduction, and Organic Photocatalysis. *J. Am. Chem. Soc.* **133**, 13445–13454 (2011).
13. Kataoka, Y. *et al.* Photocatalytic hydrogen production from water using porous material $[Ru_2(p\text{-}BDC)_2]_n$. *Energy Environ. Sci.* **2**, 397–400 (2009).
14. Wang, J.-L., Wang, C. & Lin, W. Metal–Organic Frameworks for Light Harvesting and Photocatalysis. *ACS Catal.* **2**, 2630–2640 (2012).
15. Kreno, L. E. *et al.* Metal–Organic Framework Materials as Chemical Sensors. *Chem. Rev.* **112**, 1105–1125 (2012).
16. Díaz, R., Orcajo, M. G., Botas, J. A., Calleja, G. & Palma, G. Co8-MOF-5 as electrode for supercapacitors. *Mater. Lett.* **68**, 126–128 (2012).
17. Lee, D. Y. *et al.* Unusual energy storage and charge retention in Co-based metal–organic-frameworks. *Microporous Mesoporous Mater.* **153**, 163–165 (2012).
18. Lee, D. Y. *et al.* Supercapacitive property of metal–organic-frameworks with different pore dimensions and morphology. *Microporous Mesoporous Mater.* **171**, 53–57 (2013).
19. Silva, C. G., Corma, A. & García, H. Metal–organic frameworks as semiconductors. *J. Mater. Chem.* **20**, 3141–3156 (2010).
20. Lopez, H. A. *et al.* Photochemical Response of Commercial MOFs: $Al_2(BDC)_3$ and Its Use As Active Material in Photovoltaic Devices. *J. Phys. Chem. C* **115**, 22200–22206 (2011).
21. Feldblyum, J. I., Keenan, E. A., Matzger, A. J. & Maldonado, S. Photoresponse Characteristics of Archetypal Metal–Organic Frameworks. *J. Phys. Chem. C* **116**, 3112–3121 (2012).
22. Joyce, J. T., Laffir, F. R. & Silien, C. Layer-by-Layer Growth and Photocurrent Generation in Metal–Organic Coordination Films. *J. Phys. Chem. C* **117**, 12502–12509 (2013).
23. Zhan, W.-W. *et al.* Semiconductor@Metal-Organic Framework Core–Shell Heterostructures: A Case of ZnO@ZIF-8 Nanorods with Selective Photoelectrochemical Response. *J. Am. Chem. Soc.* **135**, 1926–1933 (2013).
24. Li, Y., Pang, A., Wang, C. & Wei, M. Metal–organic frameworks: promising materials for improving the open circuit voltage of dye-sensitized solar cells. *J. Mater. Chem.* **21**, 17259–17264 (2011).
25. Zhan, W.-W. *et al.* Semiconductor@metal-organic framework core–shell heterostructures: a case of ZnO@ZIF-8 nanorods with selective photoelectrochemical response. *J. Am. Chem. Soc.* **135**, 1926–1933 (2013).
26. Sun, L.-P., Niu, S.-Y., Niu, J. J., Yang, G.-D. & Ye, L. *Eur. J. Inorg. Chem.* 5130–5137 (2006).
27. Lee, D. Y. *et al.* Cu-Based Metal-Organic Frameworks for Photovoltaic Application. *J. Phys.Chem. C* (2013) **DOI:** 10.1021/jp4079663.
28. Kongkanand, A., Domín guez, R. & Kamat, P. Single Wall Carbon Nanotube Scaffolds for Photoelectrochemical Solar Cells. Capture and Transport of Photogenerated Electrons. *Nano Lett.* **7**, 676–680 (2007).
29. Kongkanand, A. & Kamat, P. Electron Storage in Single Wall Carbon Nanotubes. Fermi Level Equilibration in Semiconductor–SWCNT Suspensions. *ACS Nano* **1**, 13–21 (2007).
30. Lee, K., Hu, C., Chen, H. & Ho, K. Incorporating carbon nanotube in a low-temperature fabrication process for dye-sensitized TiO_2 solar cells. *Sol. Energy Mater. Sol. Cells* **92**, 1628–1633 (2008).
31. Lee, T., Alegaonkar, P. & Yoo, J. Fabrication of dye sensitized solar cell using TiO_2 coated carbon nanotubes. *Thin Solid Films* **515**, 5131–5135 (2007).
32. Sawatsuk, T., Chindaduang, A., Sae-kung, C., Pratontep, S. & Tumcharern, G. Dye-sensitized solar cells based on TiO_2–MWCNTs composite electrodes: Performance improvement and their mechanisms. *Diamond Relat. Mater.* **18**, 524–527 (2009).
33. Muduli, S. *et al.* Enhanced Conversion Efficiency in Dye-Sensitized Solar Cells Based on Hydrothermally Synthesized TiO_2−MWCNT Nanocomposites. *ACS Appl. Mater. Interfaces* **1**, 2030–2035 (2009).
34. Lee, W., Lee, J., Yi, W. & Han, S.-H. Electric-Field Enhancement of Photovoltaic Devices: A Third Reason for the Increase in the Efficiency of Photovoltaic Devices by Carbon Nanotubes. *Adv. Mater.* **22**, 2264–2267 (2010).
35. Grätzel, M. Conversion of sunlight to electric power by nanocrystalline dye sensitized solar cells. *J. Photochemis. Photobiol. A.* **164**, 3–14 (2004).

Acknowledgments

This research was supported by the KIST Institutional Program (2E23964), and the Basic Science Research Program through the National Research Foundation of Korea (NRF) funded by the Ministry of Education (2013009768), Republic of Korea. One of the authors (N.K. Shrestha) is supported by The Korean Federation of Science and Technology Societies under Brain Pool program.

Author contributions

All authors contributed to results analysis and discussion. S.-H.H. developed the concept of MOF solar cell. D.Y.L. designed and conducted all experiments. C.Y.S., S.J.Y. and H.Y.L. contributed in characterization of samples. D.Y.L., W.L., N.K.S., J.K.L. and S.-H.H. discussed the results, and N.K.S. drafted the manuscript.

Additional information

Supplementary information accompanies this paper at http://www.nature.com/scientificreports

Competing financial interests: The authors declare no competing financial interests.

How to cite this article: Lee, D.Y. *et al.* Enhanced photovoltaic performance of Cu-based metal-organic frameworks sensitized solar cell by addition of carbon nanotubes. *Sci. Rep.* **4**, 3930; DOI:10.1038/srep03930 (2014).